Flávio Medeiros Seibt
Federal University of Rio Grande do Sul
Mechanical Engineering Graduate Program
Porto Alegre,
Brazil

Felipe Vannucchi de Camargo
Federal University of Rio Grande do Sul
Post-Graduation Program in Mining,
Metallurgical and Materials Engineering,
Porto Alegre,
Brazil

Elizaldo D. dos Santos
Federal University of Rio Grande
Ocean Engineering Graduate Program
Rio Grande,
Brazil

Mateus das Neves Gomes
Federal Institute of Education, Science and
Technology of Paraná
Paranaguá,
Brazil

Luiz Alberto Oliveira Rocha
University of Vale do Rio dos Sinos
Mechanical Engineering Graduate Program
São Leopoldo,
Brazil

Liércio André Isoldi
Federal University of Rio Grande
Ocean Engineering Graduate Program
Rio Grande,
Brazil

Cristiano Fragassa
University of Bologna
Department of Industrial Engineering
Bologna,
Italy

Numerical Evaluation on the Efficiency of the Submerged Horizontal Plate Type Wave Energy Converter

The high availability of energy within ocean waves is seen as an important and abundant alternative as a renewable energy source. This paper presents a numerical study of the submerged horizontal plate type wave energy converter, assessing its theoretical efficiency for several relative plate heights. The propagation and incidence of distinct wave periods through the device structure were simulated, and the device efficiency was evaluated disregarding the presence of the turbine under the plate. A total of six wave periods between 1.25 and 3.50 s with wave height of 0.06 m were considered for six different plate heights. The results allow to make theoretical recommendations on the converter performance. The multiphase Volume of Fluid model was used through a two-dimensional approach for air-water interaction and the conservation equations of mass, momentum and volume fraction transport were solved by the Finite Volume Method. The results of analysis allowed to observe that the highest relative plate height leads to enhanced submerged horizontal plate efficiencies among the simulated wave periods, as well as to identification of a theoretical device efficiency up to three times higher for larger wave periods than for shorter wave periods.

Keywords: *Computational fluid dynamics; Submerged horizontal plate; Volume of fluid; Wave energy; Energy efficiency.*

1. INTRODUCTION

The growth in global energy demand, especially in electricity, coupled with the need for conservation of natural resources and reduction of carbon emissions, has led to a diversification of the energy market, focusing on the use of renewable energy sources [1-4]. In this sense, the ocean stands out as a promising alternative source because of its large available energetic potential [5,6].

Different oceanic physical phenomena can be exploited for energy production, mainly from waves, tides, ocean currents and ocean thermal gradients [6]. According to Gunn and Stock-Williams [7], the overall available power on surface waves reaches 2.11 ± 0.05 TW, a comparable value to the worldwide average annual electricity consumption.

Regions located at latitudes between 30° and 60° typically offer attractive energetic potentials for exploitation due to their high annual average available wave energy [5,8]. Recent studies indicate that the available wave energy along the South-Southeastern Brazilian shelf can vary from 6.00 up to 22.30 kW/m [9-11]. One advantage of the wave energy is its energy density, it is expected that 15 to 20 times more energy per square meter can be provided in comparison with wind or solar energy [12,13]. Therefore, even with conservative estimates about the efficiency of wave energy converters (WECs), the prospects have been stimulating the scientific and technological research to exploit this energy resource [14-18].

There are different criteria used to classify the WECs. The two most common are the location (shoreline, near-shore and offshore) and the working principle (OWC, overtopping and oscillating bodies) [5,8]. However, these criteria do not cover all the existing possibilities of converting the wave energy into electricity, not completely and accurately describing multifunctional structures, for instance. Thus, distinct methodologies are discussed in the literature, such as the classification proposed by Margheritini et al. [2], which presents specific criteria for total characterization of WECs that allow a general environment impact assessment.

Despite its energetic potential, harvesting wave energy is a yet under-explored field, mainly due to the high cost of current technologies. In this sense, energy conversion structures that perform more than one function have been studied by the possibility of reducing installation costs, for example, WECs associated with breakwaters: oscillating water column (OWC) onshore [16], overtopping onshore [17,18] and the submerged horizontal plate (SHP) near-shore [19,20].

Received: February 2019, Accepted: April 2019
Correspondence to: Felipe Vannucchi de Camargo,
Metallurgical and Materials Engineering, Federal
University of Rio Grande do Sul, Porto Alegre, Brazil
E-mail: felipe.vannucchi@unibo.it
doi: 10.5937/fmet1903543S

The submerged horizontal plate (SHP) device is a type of structure used in coastal engineering, such as submerged breakwater, for coastal protection purposes and can also be used as a WEC [19,21,22]. The use of this structure as a WEC has the main characteristic of the double functionality of the structure, since the same device used for wave energy conversion can be used as a breakwater [20].

The SHP device consists of a single flat plate submerged at fixed depth below free surface water. The presence of the horizontal plate near the water surface tends to steepen the waves over the plate due to shoaling and part of the incident wave energy is dissipated by wave breaking, turbulence and friction on the plate [23,24]. The SHP type WEC utilizes the alternating flow below the plate, which arises due to the dissipation of the incident wave energy through the structure, acting as a propulsion for a hydraulic turbine [25,26].

This work presents a numerical study of the SHP type wave energy converter. The aim of this study is to evaluate the theoretical device efficiency for several relative plate heights and different wave periods propagating through the device structure. The device efficiency was evaluated disregarding the presence of the turbine under the plate. The results achieved allow to make theoretical recommendations about the device geometry.

A two-dimensional domain was built for a numerical model based on the multiphase model Volume of Fluid (VOF) [27,28] to simulate the air-water interaction. Conservation equations of mass and momentum are solved for all studied cases using ANSYS® Fluent which is a Finite Volume Method (FVM) [29,30] code-based software.

2. MATERIALS AND METHODS

2.1 Submerged Horizontal Plate

Initially studied as a mere breakwater, the submerged plate system began to show its potential for further applications after experiments performed by Dick and Brebner [31] with solid and permeable submerged blocks, in which the flow pattern around the permeable blocks is presented, thus demonstrating the fluid dynamic characteristics of the plate for coastal protection purposes.

Afterwards, Graw [32] described the system as an efficient wave filter, whose flow below the plate was considered advantageous over to other submerged breakwaters. In this same work, it is affirmed that this flow is quite stable, not undergoing significant changes even when the region under the plate is partially obstructed. Graw [19] announced the SHP type WEC. The author proposed the use of the stable flow under the SHP as propulsion for a hydraulic turbine (Figure 1) installed under the plate [19,25,33,34].

Graw [35] presented a study on the WECs feasibility associated with breakwaters including the SHP system in this context. Despite the potential of the SHP as a dual-function device [34,35], many of the studies on this subject are focused on its use solely as a breakwater [36-40]. These studies, however, contribute to a better understanding of the phenomena related to the flow around the SHP.

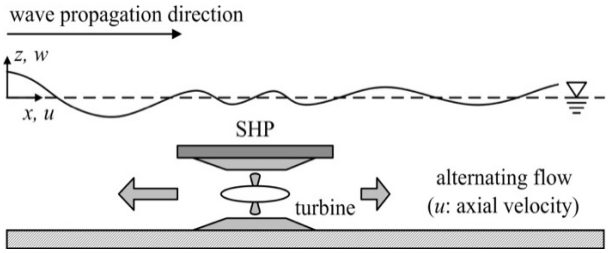

Figure 1. Sketch of the submerged horizontal plate device.

Carter [21] studied the SHP type WEC using a two-dimensional numerical model with the Boundary Element Method and the linear wave theory. This study presented the velocity field of the flow under the plate, whose results evidenced the altering behavior of the flow direction. In a later study, Carter et al. [41] compared this model with a RANS based model, concluding that there is no significant difference between the two approaches once both describe the flow behavior very similarly.

Orer and Ozdamar [26] presented an experimental evaluation of the SHP device efficiency as a WEC. In this study, the flow velocity under the plate was analyzed when the device, at a fixed height, is subjected to several incident waves. The authors indicated a theoretical efficiency around 60% for the device, in opposition to Graw [33] who had predicted an efficiency of only 4 %.

In Seibt et al. [42], a two-dimensional numerical model of the SHP device based on the FVM and VOF methods was used for describing the air-water interface. In this work, the validation of the model based on the experimental results of Orer and Ozdamar [26] was presented, from the reproduction of a case without constraints under the plate, to the verification of the model based on the free-surface elevation equation and velocity components equations from the 2nd-order Stokes theory.

Seibt et al. [43] presented a numerical study of the SHP conversion efficiency at six different plate heights in relation to the bottom. Among the results, the flow velocity profiles under the plate for each case were showed, as well as the behavior of the flow field velocity vectors over a wave period for highest efficiency case scenario. The results depicted an efficiency up to 64 % for the case where the plate was positioned closest to the water surface.

Seibt et al. [44] also presented a numerical evaluation of the influence of the area reduction under the SHP on its conversion efficiency. Configurations were analyzed with the insertion of triangular structures under the SHP, in order to reduce the area without changing the submersion depth, and compared with the case without area reduction. The results showed that the area reduction caused a growth up to 300 % in the velocities magnitudes and a decrease around 5 % in the conversion efficiency among the analyzed cases.

In Gomes et al. [45], the length of the SHP was analyzed by selecting five different plate lengths and checking the simulation outcome for a fixed depth. The results showed that the plate length variation had little influence over the SHP efficiency, which reached about 20% for all studied cases. Seibt et al. [46] presented an evaluation of the influence of some plate heights, with

fixed plate length, subjected to different wave periods on the equipment efficiency. The results showed that longer waves can lead to conversion efficiencies up to 27 % among the assessed cases.

In the present work, a set of six SHP geometries was tested for six different incident wave characteristics. Thus, allowing an evaluation on the theoretical device efficiency and the effect of the relative plate height for several incident wave conditions.

2.2 Computational Modeling

The computational model was developed with Computational Fluid Dynamics software ANSYS® Fluent, which solves the governing equations by means of the FVM. This method allows obtaining a discrete version of Partial Differential Equations (PDEs) and is based on a physical approach to the problem represented by the PDE. This method is widely used in engineering applications involving fluid dynamics, such as aerodynamics, hydrodynamics and fluid-structure interaction [30,47-49].

The conservation equations of mass and momentum for an isothermal, laminar and incompressible flow with two phases solved for the mixture of air and water are given by (1), (2) and (3) [50,51]:

$$\frac{\partial u}{\partial x}+\frac{\partial w}{\partial z}=0 \tag{1}$$

$$\rho\frac{\partial u}{\partial t}+\rho\left(u\frac{\partial u}{\partial x}+w\frac{\partial u}{\partial z}\right)=-\frac{\partial p}{\partial x}+\mu\left[\frac{\partial^2 u}{\partial x^2}+\frac{\partial^2 u}{\partial z^2}\right] \tag{2}$$

$$\rho\frac{\partial w}{\partial t}+\rho\left(u\frac{\partial w}{\partial x}+w\frac{\partial w}{\partial z}\right)=-\frac{\partial p}{\partial z}+ +\mu\left[\frac{\partial^2 w}{\partial x^2}+\frac{\partial^2 w}{\partial z^2}\right]+\rho g \tag{3}$$

where ρ is the density (kg/m³), u and w are the horizontal and vertical velocity components (m/s), respectively, p is the pressure (N/m²), ρg is the buoyancy (N/m³) and μ is the dynamic viscosity coefficient (kg/m·s). In order to represent the air-water interaction of the flow and to evaluate its interaction with the equipment, the VOF method was used. The VOF method is a multiphasic model applied to fluid flows where there are two or more immiscible phases [27,28].

In addition, the volume fraction (α), used to represent both phases inside the control volume, is assumed to be continuous in space and time in each control volume. Accordingly, there are three possible situations: i) α = 1: indicates a control volume filled only by water, ii) α = 0: indicates a control volume without water, filled only by air; iii) 0 < α < 1: identifies the free surface position, i.e. a transition region having both water and air. Thus, the volume fraction evolution for two phases in each mesh element on the computational domain obeys a transport equation given by (4) [28,52]:

$$\frac{\partial(\alpha)}{\partial t}+\frac{\partial(\alpha u)}{\partial x}+\frac{\partial(\alpha w)}{\partial z}=0 \tag{4}$$

The values of density and viscosity coefficient for the mixture can be written as (5) and (6) [28]:

$$\rho=\alpha\rho_{water}+(1-\alpha)\rho_{air} \tag{5}$$

$$\mu=\alpha\mu_{water}+(1-\alpha)\mu_{air} \tag{6}$$

Since the flow has low velocity, the fluid is assumed incompressible disregarding possible density variations for each phase, so the state equation is enough to solve the pressure at any computational cell of domain [30].

The mathematical model is complemented by the boundary conditions, which are assigned as follows: time dependent velocity (u (x, z, t); w (x, z, t)) at the left edge (bold line, representing the channel wavemaker) [53], atmospheric pressure (patm) at the upper edge and part of the left edge (dash-dot line) and non-slip and impermeability condition (u (x, z, t) = w (x, z, t) = 0) at the other edges (straight line), as seen in Figure 2.

The time dependent velocity was composed by (7) and (8) from the second order Stokes theory, for wave velocity components, in the horizontal (x) and vertical (z) directions, respectively, given as [54]:

$$u(x,z,t)=\frac{\varepsilon}{2}\left(\frac{gk}{\omega}\right)\left[\frac{\cosh k(d+z)}{\cosh(kd)}\right]\cos(kx-\omega t)+ +\frac{3}{16}\left[\frac{\varepsilon^2\omega k\cosh 2k(d+z)}{\sinh^4(kd)}\right]\cos 2k(kx-\omega t) \tag{7}$$

$$w(x,z,t)=\frac{\varepsilon}{2}\left(\frac{gk}{\omega}\right)\left[\frac{\sinh k(d+z)}{\cosh(kd)}\right]\sin(kx-\omega t)+ +\frac{3}{16}\left[\frac{\varepsilon^2\omega k\sinh 2k(d+z)}{\sinh^4(kd)}\right]\sin 2k(kx-\omega t)-\omega t \tag{8}$$

where ε is the wave height (m), g is the gravitational acceleration (g = 9.81 m/s²), k is the wave number given by k = 2π/λ (m-1), λ is the wave length (m), ω is the wave frequency given by ω = 2π/T (rad/s), T is the wave period (s), d is the water depth (m) and t is the time (s).

The wave length (λ) is defined by (9) from the second order Stokes theory, being interactively calculated by the dispersion equation [53]:

$$\lambda=\left(\frac{g}{2\pi}\right)T^2\tanh\left(\frac{2\pi}{\lambda}d\right) \tag{9}$$

The following solution parameters were utilized to set the solver: 1st-order Upwind advection scheme to the advective terms; PRESTO to spatial pressure discretization; Geo-Reconstruct to the volume fraction discretization; PISO for the pressure-velocity coupling method; sub-relaxation factors 0.3 and 0.7 for the mass and momentum, respectively. All simulations of the present work refer to a flow time of 11T (where T is the wave period) aiming to avoid the wave reflection effect. A time step of 0.001 s was used in all cases.

In order to evaluate the theoretical device efficiency, it is necessary to compute the available flow power under the SHP, i.e. the fraction of wave flow power which can be theoretically exploited and applied for the propulsion of a hydraulic turbine.

The SHP efficiency (φ) is defined by (10) as [26,55]:

$$\phi=\frac{P_p}{P_W} \tag{10}$$

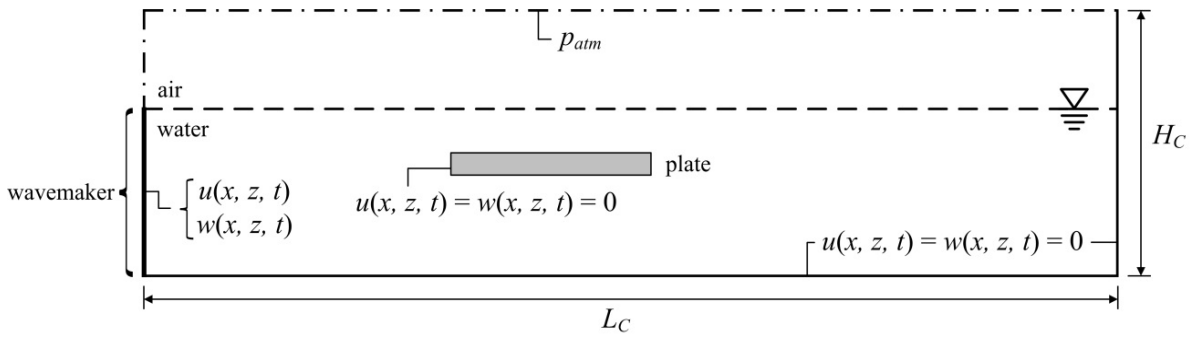

Figure 2. Computational model boundary conditions.

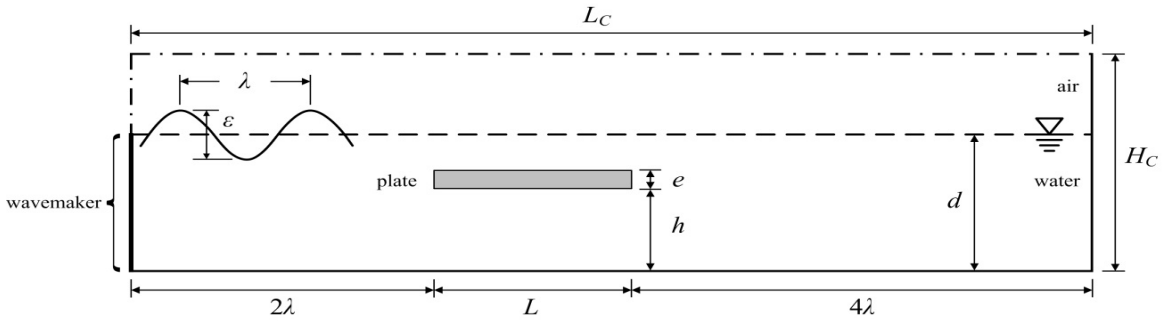

Figure 3. Computational model sketch.

where P_P is the available power under the plate (W) and P_W is the wave power that reaches the device (W), which is obtained by (11) as [56]:

$$P_W = \left(\frac{1}{16}\rho g\varepsilon^2\right)\frac{\omega}{k}\left(1+\frac{2kd}{\sinh 2kd}\right)\left[1+\frac{9}{64}\frac{\varepsilon^2}{k^4 d^6}\right] \quad (11)$$

The time-averaged available power under the plate (P_P) is calculated by (12) [21,57]:

$$P_p = \frac{1}{T}\int_t^{(t+T)}\int_{-d}^{-(d-h)}\left(p+\frac{1}{2}\rho u^2\right)\cdot u\cdot b\cdot dz\cdot dt \quad (12)$$

where p is the static pressure under the plate, the term ($\rho u^2/2$) represents the dynamic pressure and b is the plate width which is unitary in the 2D model.

In the numerical simulation of the SHP device the 2D representation of a wave channel was considered with the presence of a horizontal plate submerged below the free surface of water. According to Figure 3, the dimensions are: channel height HC = 1.00 m, channel length LC (LC = 6λ+L), plate length L = 2.50 m and water depth d = 0.60 m. It should be noted that the wave channel and plate widths were considered unitary since the numerical model is two-dimensional.

On the comparative analyses among the simulated cases, the data was surveyed using numerical probes that were inserted in the region under the plate. The main numerical probes were the central point (cp) and the line (l) (Figure 4), which monitored the horizontal velocities (u) and mass flow rate ($\dot{m}$), respectively. Furthermore, the pressure data was surveyed by the same points that monitored the velocities.

According to Figure 3, some dimensions in the numerical domain were defined based on the characteristics of each simulated wave. These dimensions were fixed as a way to guarantee minimum conditions for the wave development and propagation before reaching the plate, as well as to guarantee the incidence of some waves on the SHP before its reflection in the end of the channel (region downstream of the plate). Thus, the definition of this dimensions allows the survey of a sufficient amount of data to be analyzed.

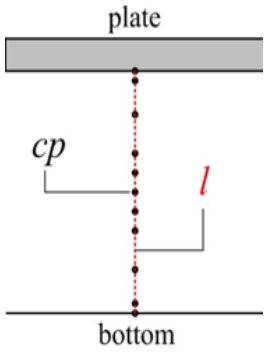

Figure 4. Location sketch of numerical probes under plate.

The mesh was built using the recommendations of Ramalhais [58], which showed to be adequate in previous studies [46]. Thus, each computational cell did not exceed λ/60 of length in the direction of wave propagation, and ε/20 of height in the region where the wave propagates, as well as at the bottom of the channel.

2.3 Problem Description

Since the dimensions of the channel and plate were fixed (apart from the channel length which is proportional to the wave length), just the plate height varied for each simulated wave. By its turn, the wave characteristics was not completely modified. The wave height and the water depth were kept fix whereas the wave period and length varied. The dimensions of the plate and wave are presented in Figure 3 where: plate length L = 2.50 m, plate thickness e = 0.02 m and wave height ε = 0.06 m.

The plate height (h) varied for six values (Table 1) which will be referred as relative plate height (X = h/d) henceforward. Thus, the analyzed plate geometries were organized as presented in Table 1.

Table 1. Set of plate geometries.

Plate	h (m)	$X = h/d$
P1	0.46	76.7 %
P2	0.48	80.0 %
P3	0.50	83.3 %
P4	0.51	85.0 %
P5	0.52	86.7 %
P6	0.53	88.3 %

Besides that, six wave periods were utilized for incident wave simulation, as shown in Table 2. The ratio λ/L to each one is also presented in Table 2.

Table 2. Set of incident wave characteristics.

Wave	ε (m)	T (s)	λ (m)	λ/L
W1	0.06	1.25	2.27	0.91
W2	0.06	1.50	3.00	1.20
W3	0.06	2.00	4.36	1.74
W4	0.06	2.50	5.67	2.27
W5	0.06	3.00	6.95	2.78
W6	0.06	3.50	8.21	3.30

In this way, each geometry was tested for several incident wave characteristics which aimed to evaluate the SHP efficiency in each condition, as well as to analyze the effect of relative plate height over the alternating water flow below the device. It should be noticed that the plate length (L = 2.50 m) was remained fixed based on previous studies carried by the authors research group [42,45,46].

3. RESULTS AND DISCUSSION

Figure 5 shows the behavior of the flow axial velocity $|-u_{max}|$ under the SHP to all simulated cases. From the surveyed data on the point cp (see Figure 4), it was accounted the maximum value acquired along the simulated flow time. Since these values occurred in opposite direction to the wave propagation, results were presented in absolute value.

In Figure 5a, there is a growth tendency for the flow axial velocity under the SHP as the wave period increases, as well as when the plate remains closer to the water surface. In addition, it was observed that the growth trend had changes for the waves W5 and W6 (λ/L > 2.27, Table 2) which are the largest simulated wave periods.

Figure 5b reinforces this general trend, however, it shows two other aspects: firstly, the wave W5 had a decrease in its maximum velocity magnitude from the minor relative plate height (X = 76.7 %) down to a minimum $|-u_{max}|$ at X = 85.00 % and showed a small increase in the maximum velocity magnitude after that point to the highest relative plate height tested (X = 88.3 %). Secondly, the wave W6 has a decrease in its maximum velocity magnitude as the plate remains closer to the water surface, over the tested range of relative plate height.

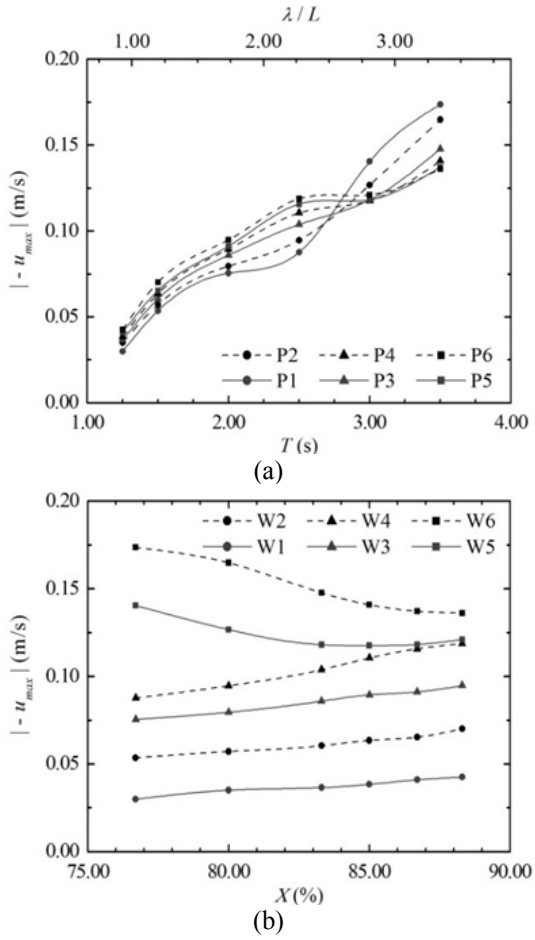

Figure 5. Flow maximum axial velocity magnitude $|-u_{max}|$ to: (a) wave periods T, (b) relative plate heights X.

The mean increase observed in the maximum velocity magnitude (Figure 5) from the smallest to the largest wave periods was around 3.5 times. In this sense, there is a trend that larger wave periods led to highest flow axial velocity magnitudes. From the viewpoint of wave energy conversion, this is an important information since it refers to the turbine rotation characteristics.

Figure 6 shows the behavior of the mass flow rate $\dot{m}_{RMS}$ under the SHP to all simulated cases. From the monitored data on the line l, the root mean square (RMS) was accounted for the values acquired along the simulated flow time. Since the water flow has alternating direction (positive and negative values), its results were represented by RMS value.

In Figure 6a, a growth tendency for the mass flow rate $\dot{m}_{RMS}$ under the SHP can also be observed as the wave period increases and as the plate approaches to the water surface. This trend was expected as X increases, since the area under the plate also increases allowing more fluid to pass through the SHP. Furthermore, particular features were noted for the waves W5 and W6 (λ/L > 2.27).

Figure 6b shows the same general trend for the results, agreeing with Fig. 6a as expected, and shows the trend changes occurred for the waves W5 and W6. For W5, initially, as the plate is placed closer to the water surface, $\dot{m}_{RMS}$ decreases down to a minimum value at X = 83.3 %, and thereafter an increase that reached to a maximum value at X = 88.3 %. Similarly

to W5, for W6 there is a decrease in $\dot{m}_{RMS}$ as the plate was approaches the water surface down to a minimum value at X = 85.0 %, and thereafter a small increase in $\dot{m}_{RMS}$. Unlike for W5, in W6 the maximum value for $\dot{m}_{RMS}$ occurred at X = 76.7 %.

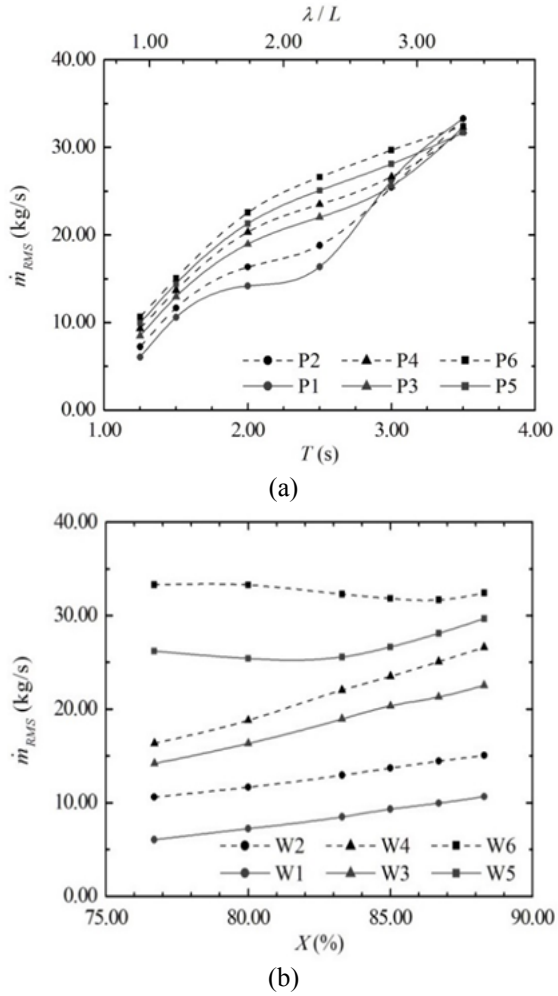

Figure 6. Mass flow rate $\dot{m}_{RMS}$ to: (a) wave periods T, (b) relative plate heights X.

Besides, it should be noted that the increase in mass flow rate $\dot{m}_{RMS}$ (Figure 6) from the smallest wave period to the largest wave period was around 4.0 times.

In order to evaluate the influence of the incident wave characteristics over the SHP efficiency, it is necessary to analyze the wave power for each wave. In Figure 7, there is an increase in the wave power of around 2.0 times as the wave period increases. From Equation 11 and Table 2, it can be observed that the growth on wave power is due to wave length (L) increase, which is an inner term of wave number (k).

The efficiency curves (φ) results are shown in Figure 8. Similar to what was observed in Figures 5 and 6, the theoretical SHP efficiency also exhibits an upward general trend as the wave period increases and as the plate is placed closer to the water surface.

In Figure 8a, the growth trend observed in SHP efficiency as the wave period increases was expected since the wave power enhances concomitantly (Figure 7). However, two other aspects must be considered: firstly, the geometry X = 88.3 % (P6) led to higher SHP efficiencies for all simulated wave periods among tested geometries. Secondly, disregarding the curve P6, two congruence regions may be observed at T = 1.25 s (λ/L = 0.91) and T = 3.50 s (λ/L = 3.30) which points to the effect of plate length on the wave length (λ/L), i.e. waves shorter than the plate are dissipated over the SHP, on the other hand, waves longer than the plate do not dissipate so easily [34].

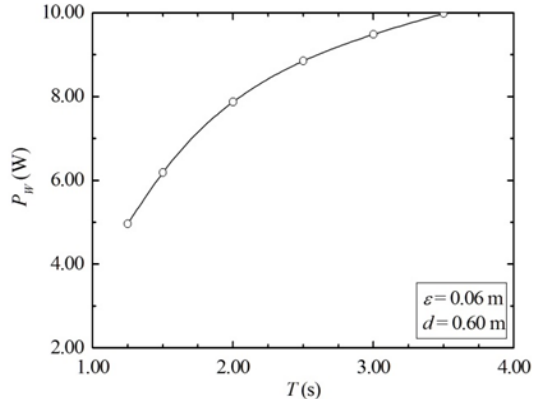

Figure 7. Wave power P_W for each incident wave period T.

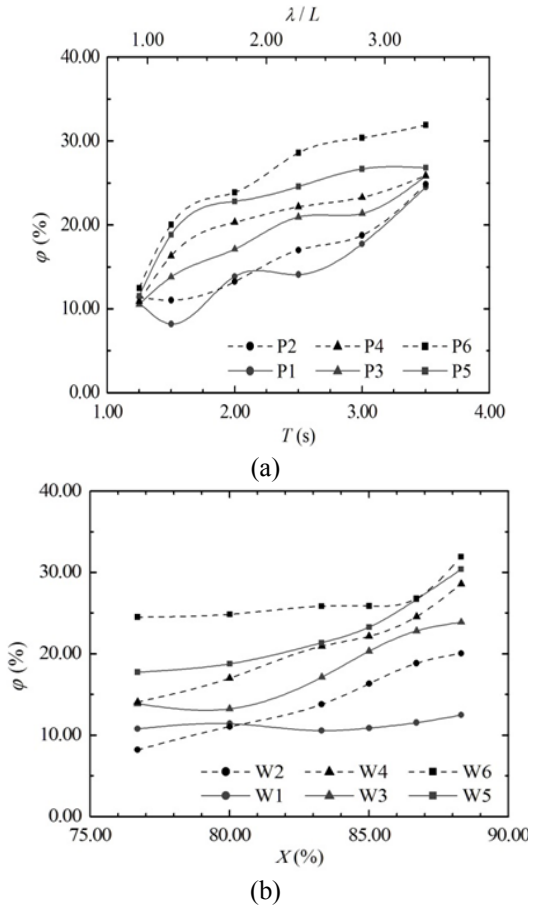

Figure 8. Theoretical SHP efficiency φ to: (a) wave periods T, (b) relative plate heights X.

The aspects shown in Figure 8a are reinforced by Figure 8b, since for the curves W1 (T = 1.25 s) and W6 (T = 3.50 s), in the range from X = 76.7 % up to X = 86.7 %, there is little variation to SHP efficiency values. In addition, the mean increase in SHP efficiency is of about 2.5 times whereas the overall increase between the lowest value and the highest value is around 4.0 times among the simulated cases.

4. CONCLUSIONS

This numerical study evaluated the theoretical SHP efficiency and the influence of the relative plate height and wave characteristics on its performance. The computational domain disregarded the presence of a hydraulic turbine under the plate in this evaluation. Besides the simulated SHP geometries, six incident wave periods in the range from 1.25 s up to 3.50 s were regarded in these analyses.

The assessment of flow parameters $| - u_{max}|$ and $\dot{m}_{RMS}$ allowed to note the wave power as dominant parameter over the flow characteristics and over the SHP efficiency (φ), which was already expected. However, the length ratio λ/L also demonstrated its importance, since the length ratios λ/L > 2.27 had higher efficiency gains than others. On the other hand, the increase of the relative plate height X led to an increase in the SHP efficiency values, despite the decrease in $| - u_{max}|$ which happened to Waves 5 and 6.

Along the result analysis, it was verified that, from the lowest to the highest wave powers (T = 1.25 s and T = 3.50 s, respectively), there were increases for the flow maximum axial velocity magnitude $| - u_{max}|$ of around 250 % and for the mass flow rate $\dot{m}_{RMS}$ of about 300 %, whereas the increase in wave power was up to 100 % for the range of analyzed wave periods. Regarding the theoretical SHP efficiency, its increase was approximately 24 % and the best performance reached was φ = 31.9 %.

In future studies, other SHP geometries will be analyzed to widen this evaluation, as well as other methods will be applied in order to improve the search for a geometry that provides the best device performance attainable, such as Constructal Design [59].

ACKNOWLEDGMENT

This research was funded by the National Council for Scientific and Technological Development of the Brazilian Ministry of Science, Technology, Innovation and Communications (CNPq/MCTIC) (Grants: 306024/2017-9, 306012/2017-0, 307847/2015-2), the Coordination of Improvement of Higher Education Personnel of the Brazilian Ministry of Education (CAPES/MEC) and the Foundation for Research Support of Rio Grande do Sul (FAPERGS). F.M. Seibt and F.V. de Camargo thank respectively CNPq and CAPES for the doctorate scholarships.

REFERENCES

[1] Pelc, R., Fujita, R.M.: Renewable energy from the ocean. Marine Policy, Vol. 26, pp. 471-479, 2002.

[2] Margheritini, L., Hansen, A.M. and Frigaard, P.: A method for EIA scoping of wave energy converters – based on classification of the used technology. Environ. Imp. Assess. Rev., Vol. 32, pp. 33-44, 2012.

[3] Minak, G., Fragassa, C. and de Camargo, F.V.: A brief review on determinant aspects in energy efficient solar car design and manufacturing. In *International Conference on Sustainable Design and Manufacturing*, Springer: Cham, Switzerland, 26-28 April 2017, pp. 847-856.

[4] Zampiva, R.Y.S. et al.: Mg2SiO4: Er3+ Coating for Efficiency Increase of Silicon-Based Commercial Solar Cells. In *International Conference on Sustainable Design and Manufacturing (SDM 2017)*, Bologna, Italy, 26-28 April 2017, Springer: Cham, Switzerland, pp. 820-828.

[5] Falcão, A.F.O.: Wave energy utilization: A review of the Technologies. Renew. Sustainable Energy Rev., Vol. 14, pp. 899-918, 2010.

[6] Uihlein, A. and Magagna, D.: Wave and tidal current energy – A review of the current state of research beyond technology. Renew. Sustainable Energy Rev., Vol. 58, pp. 1070-1081, 2016.

[7] Gunn, K. and Stock-Williams, C.: Quantifying the global wave power resource. Renew. Energy, Vol. No. 44, pp. 296-304, 2012.

[8] Cruz, J.: *Ocean wave energy: current status and future perspectives*. Springer-Verlag: Berlin, Germany, 2008.

[9] Contestabile, P., Ferrante, V. and Vicinanza, D.: Wave Energy Resource along the Coast of Santa Catarina (Brazil). Energies, Vol. 8, pp. 14219-14243, 2015.

[10] Oleinik, P.H., Marques, W.C. and Kirinus, E.P.: Evaluation of the Seasonal Pattern of Wind-Driven Waves on the South-Southeastern Brazilian Shelf. Defect Diffus. Forum, Vol. 370, pp. 141-151, 2016.

[11] Lisboa, R.C., Teixeira, P.R.F. and Fortes, C.J.: Numerical evaluation of wave energy potential in the south of Brazil. Energy, Vol. 121, pp. 176-184, 2017.

[12] Rasuo, B., Dinulovic, M., Veg, A., Grbovic, A., Bengin, A.: Harmonization of new wind turbine rotor blades development process: A review, Renewable and Sustainable Energy Reviews, Vol. 39, pp. 874-882, 2014.

[13] Rasuo, B., Bengin, A.: Optimization of Wind Farm Layout, FME Transactions, Vol. 38 No. 3, pp 107-114, 2010.

[14] Rasuo, B., Bengin, A., Veg, A.: On Aerodynamic Optimization of Wind Farm Layout, PAMM, Vol. 10, No. 1, pp. 539–540, 2010.

[15] Son, D., Belissen, V. and Yeung, R.W.: Performance validation and optimization of a dual coaxial-cylinder ocean-wave energy extractor. Renew. Energy, Vol. 92, pp. 192-201, 2016.

[16] Falcão, A.F.O. and Henriques, J.C.C.: Oscillating-water-column wave energy converters and air turbines: A review. Renew. Energy, Vol. 85, pp. 1391-1424, 2016.

[17] Margheritini, L., Vicinanza, D. and Frigaard, P.: SSG wave energy converter: Design, reliability and hydraulic performance of an innovative overtopping device. Renew. Energy, Vol. 34, pp. 1371-1380, 2009.

[18] Vicinanza, D., Contestabile, P., Nørgaard, J.Q.H. and Andersen, T.L.: Innovative rubble mound breakwaters for overtopping wave energy conversion. Coast. Eng., Vol. 88, pp. 154-170, 2014.

[19] Graw, K.-U.: Shore protection and electricity by submerged plate wave energy converter. In *Proceedings of the European Wave Energy Symposium, Edinburgh*, Scotland, 21-24 July 1993, Elliot, G., Caratti, G., Eds., pp. 379-384.

[20] Ning, D., Li, Q., Lin, H. and Teng, B.: Numerical Investigation of Nonlinear Wave Scattering by a Horizontal Submerged Plate. Procedia Eng., Vol. 116, pp. 237-244, 2015.

[21] Carter, R.W.: *Wave energy converters and a submerged horizontal plate*. MSc thesis, University of Hawaii at Manoa, Honolulu, HI, USA, 2005.

[22] Brossard, J., Perret, G., Blonce, L. and Diedhiou, A.: Higher harmonics induced by a submerged horizontal plate and a submerged rectangular step in a wave flume. Coast. Eng., Vol. 56, pp. 11-22, 2009.

[23] Teh, H.M.: Hydraulic performance of free surface breakwaters: A review. Sains Malaysiana, Vol. 42, pp. 1301-1310, 2013.

[24] Wang, G., Ren, B., Wang, Y.: Experimental study on hydrodynamic performance of arc plate breakwater. Ocean Eng., Vol. 111, pp. 593-601, 2016.

[25] Graw, K.-U.: Device for generating electrical energy from water waves. PINA (Patent- und Innovationsagentur des Landes Nordrhein-Westfalen), German Patent Nr. P4324110, 1995.

[26] Orer, G. and Ozdamar, A.: An experimental study on the efficiency of the submerged plate wave energy converter. Renew. Energy, Vol. 32, pp. 1317-1327, 2007.

[27] Hirt, C.W. and Nichols, B.D.: Volume of fluid (VOF) method for the dynamics of free boundaries. J. of Comp. Phys., Vol. 39, pp. 201-225, 1981.

[28] Srinivasan, V., Salazar, A.J. and Saito, K.: Modeling the disintegration of modulated liquid jets using volume-of-fluid (VOF) methodology. Appl. Math Model., Vol. 35, pp. 3710-3730, 2011.

[29] Patankar, S.V.: *Numerical heat transfer and fluid flow*. McGraw Hill: New York, NY, USA, 1980.

[30] Versteeg, H.K. and Malalasekera, W.: *An introduction to computational fluid dynamics – the finite volume method*. Pearson: London, UK, 2007.

[31] Dick, T.M. and Brebner, A.: Solid and Permeable Submerged Breakwaters. In *Proceedings of the 11th Conference on Coastal Engineering (ICCE Conference Proceedings)*, London, UK, 1968, O'Brien, M.P., Ed., ASCE Publishing: New York, NY, USA, pp. 1141-1158, 1969.

[32] Graw, K.-U.: The Submerged Plate as a Wave Filter: The Stability of the Pulsating Flow Phenomenon. In *Proceedings of the 23rd Conference on Coastal Engineering, (ICCE Conference Proceedings)*, Venice, Italy, 4-9 October 1992, Edge, L.B., Ed., ASCE Publishing: New York, NY, USA, pp. 1153-1160.

[33] Graw, K.-U.: The submerged plate wave energy converter: A new type of wave energy device. *In Proceedings of International Symposium on Ocean Energy Development (ODEC)*, Muraro, Hokkaido, Japan, 1993, pp. 307-310.

[34] Graw, K.-U.: Is the submerged plate wave Energy converter ready to act as a new coastal protection system? In *Proceedings of the 24th Convegno di Idraulica e Costruzioni Idrauliche*, Naples, Italy, 20-22 September 1994, pp. 1-9.

[35] Graw, K.-U.: *About the development of wave energy breakwaters*. LACER – Leipzig Annual Civil Engineering Report Nº 1, 1996.

[36] Hsu, H.H. and Wu, Y.C.: Scattering of water wave by a submerged horizontal plate and a submerged permeable breakwater. Ocean Eng., Vol. 26, pp. 325-341, 1998.

[37] Brossard, J. and Chagdali, M.: Experimental investigation of the harmonic generation by waves over a submerged plate. Coast. Eng., Vol. 42, pp. 277-290, 2001.

[38] Liu, C., Huang, Z. and Tan, S.K.: Nonlinear scattering of non-breaking waves by a submerged horizontal plate: Experiments and simulations. Ocean Eng., Vol. 36, pp. 1332-1345, 2009.

[39] Lin, H.X., Ning, D.Z., Zou, Q.P., Teng, B., Chen, L.F.: Current effects on nonlinear wave scattering by a submerged plate. J. Waterw. Port. Coast. Ocean Eng., Vol. 140, No. 04014016, pp. 1-12, 2014.

[40] Cheng, Y., Ji, C., Ma, Z., Zhai, G. and Oleg, G.: Numerical and experimental investigation of nonlinear focused waves-current interaction with a submerged plate. Ocean Eng., Vol. 135, pp. 11-27, 2017.

[41] Carter, R.W., Ertekin, R.C. and Lin, P.: On the reverse flow beneath a submerged plate due to wave action. In *Proceedings of the 25th International Conference on Offshore Mechanics and Arctic Engineering (OMAE 2006)*, Hamburg, Germany, 4-9 June 2006, ASME Publishing: New York, NY, USA, 2006, pp. 595-602.

[42] Seibt, F.M. et al.: Computational Modeling of the Submerged Plate Wave Energy Converter. *In Proceedings of the 14th Brazilian Congress of Thermal Sciences and Engineering (ENCIT)*, Rio de Janeiro, Brazil, 18-22 November 2012, Alves, L., Sphaier, L.A., Eds., American Society of Thermal and Fluids Engineers, Volume 1, pp. 1-7.

[43] Seibt, F.M., Couto, E.C., Dos Santos, E.D., Isoldi, L.A., Rocha, L.A.O. and Teixeira, P.R.F.: Numerical study on the effect of submerged depth on the horizontal plate wave energy converter. China Ocean Eng., vol. 28, pp. 687-700, 2014.

[44] Seibt, F.M., Couto, E.C., Teixeira, P.R.F., et al.: Numerical Analysis of the Fluid-Dynamic Behavior of a Submerged Plate Wave Energy

Converter. Comp. Therm. Sci: Int J., Vol. 6, pp. 525-534, 2014.

[45] Gomes, M.N. et al.: Numerical approach of the main physical operational principle of several wave energy converters: oscillating water column, overtopping and submerged plate. Defect Diffus. Forum, Vol. 362, pp. 115-171, 2015.

[46] Seibt, F.M. et al.: Numerical Evaluation of the Effect of Relative Height Variation of a Sea Wave Energy Converter Type Submerged Plate [In Portuguese]. Revista de Engenharia e Tecnologia, Vol 7, pp. 102-115, 2015.

[47] de Camargo, F.V: Survey on Experimental and Numerical Approaches to Model Underwater Explosions. J. Mar. Sci. Eng., Vol. 7, pp. 15, 2019.

[48] Ghazanfari, S.A. and Wahid, M.A.: Heat Transfer Enhancement and Pressure Drop for Fin-and-Tube Compact Heat exchangers with Delta Winglet-Type Vortex Generators. Facta Universitatis, Series: Mech. Eng., Vol. 16, No. 233-247, 2018.

[49] Vukic, M.V. et al.: 3D numerical simulations of the thermal processes in the shell and tube heat exchanger. Facta Universitatis, Series: Mech. Eng., Vol. 11, pp. 169-180, 2014.

[50] Schlichting, H. and Gersten, K.: *Boundary-layer theory*. Springer: Berlin, Germany, 2000.

[51] Meier, G.E.A. et al. (Eds.): IUTAM Symposium on One Hundred Years of Boundary Layer Research, Springer Verlag, Berlin, 2006.

[52] Gopala, V.R., van Wachem, B.G.M.: Volume of fluid methods for immiscible-fluid and free-surface flows. Chem. Eng. J., Vol. 141, pp. 204-221, 2008.

[53] Horko, M.: *CFD optimisation of an oscillating water column energy converter*. MSc thesis, University of Western Australia, Perth, 2007.

[54] Dean, R.G., Dalrymple, R.A.: *Water Wave Mechanics for Engineers and Scientists*. World Scientific Publishing Co. Pte. Ltd.: Singapore, 1991.

[55] Graw, K.-U.: Wave Energy: the hydromechanics analysis [in German]. Institut für Grundbau, Abfall- und Wasserwesen, Bergische Universitaet – Gesamthochschule Wuppertal, 1995.

[56] McCormick, M.E.: *Ocean Wave Energy Conversion*. Dover Publications, Inc.: Mineola, NY, USA, 1981.

[57] Dizadji, N., Sajadian, S.E.: Modeling and optimization of the chamber of OWC system. Energy, Vol. 36, pp. 2360-2366. 2011.

[58] Ramalhais, R.S.: *Numerical study of an oscillating water column type wave energy conversion device* [In Spanish]. MSc thesis, University Nova de Lisboa, Lisboa, Portugal, 2011.

[59] Bejan, A. and Lorente, S.: *Design with Constructal Theory*. Wiley: Hoboken, USA, 2008.

NOMENCLATURE

u	horizontal velocity component
w	vertical velocity component
x,z	cartesian coordinates
t	time
p	pressure
g	gravitational acceleration
k	wave number, $k = 2\pi/\lambda$ (m-1)
T	wave period
d	water depth
Pp	available power under the plate
Pw	wave power that reaches the device
b	plate width
h	plate height
L	plate length
$\dot{m}$	mass flow rate
X	relative plate height, $X = h/d$

Greek symbols

ρ	density
μ	dynamic viscosity coefficient
α	volume fraction of phases in a volume
ε	wave height
λ	wave length
ω	wave frequency, $\omega = 2\pi/T$
φ	efficiency of the submerged horizontal plate

НУМЕРИЧКА ПРОЦЕНА ЕФИКАСНОСТИ ПОТОПЉЕНЕ ХОРИЗОНТАЛНЕ ПЛОЧЕ КОНВЕРТОРА ЕНЕРГИЈЕ ТАЛАСА

Ф. Медеирос Сеибт, Ф.В. де Камарго, Е.Д. Дос Сантос, М.Д.Н. Гомес, Л.А.О. Роча, Л.А. Изолди, К. Фрагаса

Висока доступност енергије у океанским таласима се сматра важном и обилном алтернативом као обновљивим изворима енергије. У овом раду је приказана нумеричка студија потопљене хоризонталне плоче конвертора енергије таласног типа, процењујући његову теоријску ефикасност за неколико релативних висина плоча. Симулирано је ширење и учесталост различитих периода таласа кроз структуру уређаја, те је оцењена ефикасност уређаја без обзира на присуство турбине испод плоче. За шест различитих висина плоча разматрано је укупно шест периода таласа између 1.25 и 3.50 с висином таласа од 0.06 м. Добијени резултати омогућавају да се дају теоријске препоруке о перформансама претварача. Модел вишефазног волумена флуида коришћен је кроз дводимензионални приступ за интеракцију ваздух-вода, а конзервационе једначине транспорта масе, момента и запремине фракције решене су методом коначне запремине. Анализа резултата је показала да највиша релативна висина плоче доводи до повећане ефикасности потопљене хоризонталне плоче између симулираних периода таласа, као и да идентификује ефикасност теоретског уређаја до три пута више за веће периоде таласа него за краће периоде таласа.